

Journal of Materials and Engineering Structures

Research Paper

Correlation between the tribology of concrete and the rheology of the corresponding mortars

Amina Belaidi^{a,}, Mohammed Amine Boukli Hacene^a, El-Hadj Kadri^b, Omar Taleb^a*

^a *Laboratory EOLE, University of Tlemcen, BP 230-13000 Chetouane, Tlemcen, Algeria.*

^b *Laboratory L2MGC, University of Cergy-Pontoise, 33 boulevard du Port, 95011 Cergy-Pontoise, France.*

ARTICLE INFO

Article history:

Received : 14 December 2020

Revised : 8 April 2021

Accepted : 9 April 2021

Keywords:

Concrete

Mortar

Rheology

Tribology

ABSTRACT

The present work aims to study the possibility of characterizing the pumpability of concrete from the rheology of the derived mortars, i.e. concrete mortar (CM) and concrete equivalent mortar (CEM). As concrete is a material that is heavier than mortar, it is better to carry out tests on mortar. To this end, two test campaigns are presented in this article; the first campaign concerns the formulation of admixed concrete based on two mineral additions, namely limestone fillers and blast furnace slag. The aim of this first campaign was to study the tribological behavior of the formulated concretes. In the second test campaign, the formulations of the mortars were derived from the formulations of the corresponding concretes. Afterwards, a rheological study was carried out on these mortars. Analysis of the results obtained showed that there is a good correlation between the developed concretes and their corresponding CEMs, with fairly high determination coefficients.


1 Introduction

In order to predict the pumpability of concrete and avoid blockage problems during its placement by pumping, some research has proposed to make preliminary tests on concrete samples by examining their tribological behavior only. These tests can be performed in the laboratory or on site, thanks to the development of measuring devices, called tribometers, which are reliable, simple and easy to handle.

On the other hand, as concrete is a material that is heavier than mortar, it has proven useful and necessary to use rapid test methods capable of providing results that may be correlated with those which would be obtained on concrete. To this end, the

* *Corresponding author.*

E-mail address: a_belaidi@hotmail.com

e-ISSN: 2170-127X, 

correlation between the flow parameters of concrete and those of associated mortars has been the subject of several studies [1, 2]. P. Banfill [1] found a good relationship between the properties of fresh concrete and those of mortars containing sand particles less than 2 mm in size. Likewise, A. Yahia et al [2] proposed a relation between the spreading of a self-compacting concrete (SCC) and its corresponding mortar. In addition, other studies suggested that the rheology of concrete and that of its equivalent mortar are closely linked [3-8]. For example, J. E. Wallevik [4] proposed an empirical linear relationship between the elastic limit of concrete and that of mortar for concrete mixtures prepared with a fixed volume of coarse aggregate.

For the purpose of implementing this approach, several ways that allow obtaining mortars from a type of composition of concrete have been reported so far. The first way consists in formulating a concrete mortar (CM) starting from the initial composition of concrete by removing a quantity of gravel while preserving the initial volume of concrete; as for the second manner, it consists of formulating a concrete equivalent mortar (CEM) by replacing the gravel of concrete by sand whose surface area is equal to that of the previously removed gravel.

The concrete equivalent mortar (CEM) approach was originally developed by A. Schwartzenruber et al [9]; this method made it easier to select the admixtures during the formulation of concrete based on tests conducted on mortar instead of concrete. The validity of this method has been confirmed by numerous investigations and applications in recent years. To this end, it is useful to cite the research study carried out by J. Assaad et al [10] and J. Assaad et al [11], who showed that good correlations exist between the thixotropy of self-compacting concrete (SCC) and that of the corresponding concrete equivalent mortar (CEM). Likewise, T.K. Erdem et al [12] conducted a similar study to determine the dosage of concrete with superplasticizer based on that of the corresponding concrete equivalent mortar (CEM). The results found by these researchers also revealed that there is a relationship between the yield stress, plastic viscosity and thixotropy of concrete, on one side, and their corresponding *concrete equivalent mortars* (CEMs), on the other. However, H. D. Le et al [13] indicated that the correlation between the spreading and V-funnel flow time of self-compacting concrete and its concrete equivalent mortar (CEM) can be established only after introducing the excess paste theory.

With regard to concrete pumping, M. Adjoudj et al [14] compared the rheological characteristics of concrete, *concrete equivalent mortar* (CEM) and the boundary layer that forms at the interface between concrete and the pumping pipe walls. Note that the purpose of this comparison was to confirm that the composition of the boundary layer is different from that of *concrete equivalent mortar* (CEM). In this study, the concrete equivalent mortars (CEMs) were fabricated with fresh concrete passed through a 4 mm sieve. However, although bibliographic research has shown that it is possible to study the rheological behavior of concrete through the use of mortars, based on the correlations found between the characteristics of these two materials in the fresh state, to the best of our knowledge, no study has been conducted on the possible relationship that could exist between the tribological parameters of concrete and those of the corresponding mortars (CM and CEM). Therefore, it was deemed necessary to explore this point based on further testing, using a mortar rheometer and a concrete tribometer.

The purpose of the present work is to know whether it is possible to characterize the pumpability of concrete based on the rheological characteristics of these derived mortars (concrete mortar and concrete equivalent concrete). To achieve this objective, it was decided to study the tribological behavior of concretes and also investigate the rheological behavior of their corresponding mortars. For this, two types of mineral additions were used for the formulation of concrete, namely limestone fillers and blast furnace slag, in addition to a third generation superplasticizer based on polycarboxylate.

2 Materials and methods used

In the following section, the main characteristics of the materials used in our study as well as all the experimental approaches applied are presented. The purpose sought *to be achieved* consists in determining the rheological parameters (yield stress and viscosity) of the mortars as well as the tribological parameters of the concretes (interface yield stress and viscous constant).

2.1 Sample formulation and material characterization

The concrete and mortar samples tested consist of crushed sand (S) of class 0/4 which has a water absorption coefficient of 1.65%, a modulus of fineness equal to 2.63, an absolute density of 2.7 and compactness of 0.688. The cement used is of type CPJ CEM II / A 42.5 (C) which has a specific Blaine surface of 3598 cm² / g. In addition, two mineral additions were integrated into the composition of the mixtures under study, namely limestone fillers (F) with a specific Blaine surface equal to 3200 cm² / g, and blast furnace slag (L) with a Blaine specific surface equal to 4000 cm² / g. Table 1 gives the chemical analysis of

various binders used. In addition, it was decided to incorporate a high water reducer superplasticizer (SP) based on polycarboxylate. An optimum dosage of SP is used to formulate our samples (saturation dosage) because an excess dosage of SP can cause harmful secondary phenomena on behavior of concrete [15] or mortar [16]. This dosage representing 0.5% of the binder weight. Analysis by scanning electron microscopy (SEM) of the cement and mineral additions is represented in Fig. 1, 2 and 3. With regard to cement, Fig. 1 indicates the presence of different structures, with irregular shapes and ribs. In addition, limestone fillers are in the form of a non-abrasive powder characterized by a rhombohedral structure (Fig. 2). Figure 3 suggests that the particles of blast furnace slag exhibit a heterogeneous surface that includes rods of different sizes.

Table 1 - Chemical composition of cement, limestone fillers and blast furnace slag.

Composition	Cement	Limestone fillers (%)	Blast furnace slag (%)
SiO ₂	12,17	0,06	38.3
Al ₂ O ₃	6,18	0,29	8.81
Fe ₂ O ₃	3.61	0,22	0.98
CaO	59,45	52,63	39.63
MgO	1.05	0,84	5.54
K ₂ O	0.49	0,01	0.59
Na ₂ O	0.19	0,08	0.13
SO ₃	3.63	0,02	1.35
LOI	2,62	42,77	1
P ₂ O ₅	0,18	0,02	0.1
TiO ₂	0,43	0,02	0.42

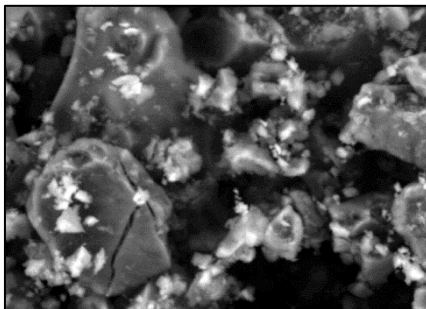


Fig. 1 – Observation of cement by the scanning electron microscope (SEM) ($\times 5000$).

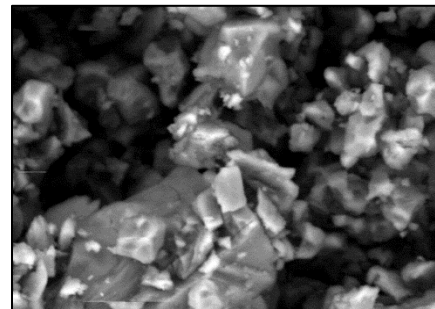


Fig. 2– Observation of limestone fillers by the scanning electron microscope (SEM) ($\times 5000$).

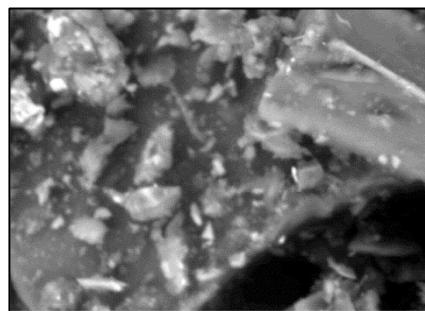


Fig. 3– Observation of blast furnace slag by the scanning electron microscope (SEM) ($\times 5000$).

The gravel types G1, G2 and G3 used in concrete belongs to the granular classes 4/8, 8/16 and 16/20, respectively. Gravel G1 has a water absorption coefficient of 1.3%, a density of 2.6 and a compactness of 0.57. Gravel G2 has an absorption coefficient of 0.5%, a density of 2.59 and a compactness of about 0.56. As for gravel G3, it has a water absorption coefficient equal to 0.77%, a density of 2.25 and a compactness of about 0.54. The size distribution of aggregates, cement, limestone fillers and blast furnace slag is illustrated in Fig. 4.

In this study, ordinary concretes were first formulated to study their tribological behaviors. To do this, the composition of a reference concrete (RC) was first determined by the Dreux-Gorisse method, and was then optimized using the Baron-Lesage method [17]. Based on this reference concrete, a mass substitution of cement was carried out with variable proportions of each mineral addition. These proportions were 10, 20, and 30% for limestone fillers, and 20, 40, and 60% for blast furnace slag (Table 2). The compositions of concrete mortars (CM) were determined based on different formulations of concrete defined above while removing the gravel of types G1, G2 and G3. The formulations of the different concrete equivalent mortars (CEMs) were determined based on the work of A. Schwartzentruber et al [9]. This operation consists of replacing the three types of gravel with a type of sand (S) that has the same surface area.

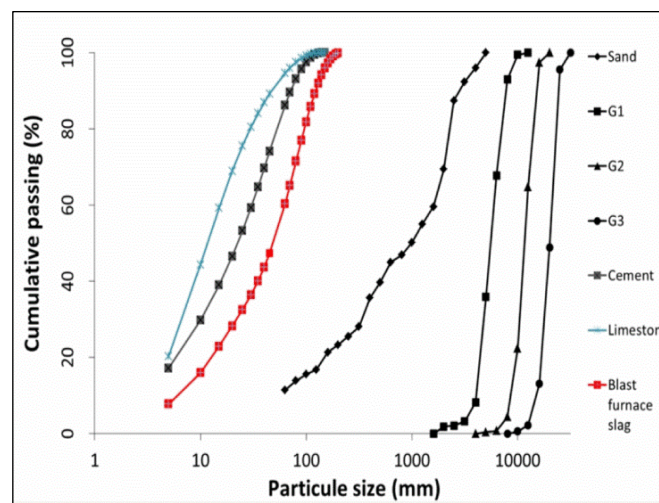


Fig. 4–Particle size distributions of aggregates, cement, limestone fillers and blast furnace slag.

Table 2 - Concrete formulations.

	RC	C1	C2	C3	C4	C5	C6
Cement (Kg/m ³)	350	315	280	245	280	210	140
Limestone fillers (Kg/m ³)	0	35	70	105	-	-	-
Blast furnace slag (Kg/m ³)	0	-	-	-	70	140	210
Sand (Kg/m ³)	660	660	660	660	660	660	660
G ₁ (Kg/m ³)	144	144	144	144	144	144	144
G ₂ (Kg/m ³)	432	432	432	432	432	432	432
G ₃ (Kg/m ³)	533	533	533	533	533	533	533
Water (l/m ³)	175	175	175	175	175	175	175
Superplasticizer (Kg/m ³)	1,75	1,75	1,75	1,75	1,75	1,75	1,75

On the other hand, Tables 3 and 4 present the surfaces area of the gravel mixture and sand, respectively. The first two columns of these tables provide the diameters of sieves of a granular range that is limited by an upper sieve T M_i (Column 1)

and by a lower sieve $T m_i$ (Column 2). Column 3 presents the diameters (d_i) of the average particle in each granular range; they are calculated using eq. (1):

$$d_i = \frac{(T M_i + T m_i)}{2} \quad (1)$$

The mass of particles in each granular interval (Mu_i) is reported in the fourth column. The unit volume (v_i) and the surface area (s_i) of the average particle in each range are grouped in columns (5) and (6), respectively. These two parameters are determined by eqs. (2) and (3).

$$V_i = \frac{\pi d_i^3}{6} \quad (2)$$

$$S_i = \pi d_i^2 \quad (3)$$

Furthermore, the mass volume of the aggregate is calculated by eq. (4) using the aggregate density (column 7).

$$\omega = \frac{1}{\mu_g} \quad (4)$$

Furthermore, the total volume of all the particles in each granular range, given in column (8), represents the product of the mass of particles in the granular range (column 4) by the mass volume of the aggregate (column 7).

Moreover, the average numbers of particles in each granular range are presented in column (9); they are obtained as the ratio between the total volume of all the particles in the granular range (column 8) and the unit volume of the average particle (column 5).

Column (10) groups the values of the surface area by the average particles in each granular range. These values are calculated by multiplying the surface area of an average particle (column 6) by the number of average particles (column 9).

The sum of all the areas calculated for each granular range (column 10) represents the surface area of the sample (see column 11). The quantity of sand (S') that replaces the gravels G_1 , G_2 and G_3 is calculated by means of eq. (5). The constituents of concrete mortar (CM) and concrete equivalent mortar (CEM) are listed in Table 5.

$$S' = \frac{SD_G \times M_G}{SD_S} \quad (5)$$

Where SD_G and SD_S are the surfaces area of gravel and sand, respectively; M_G is the total mass of all gravels.

2.2 Characterization tests for the concretes under study

2.2.1 Slump test

Concrete slump was evaluated using the Abrams cone according to standard NF P18-451.

2.2.2 Tribological test

Tribological measurements made it possible to study the behavior of concretes when they are in contact with a pumping pipe. These measurements consist in determining two essential parameters, namely the interface yield stress (τ_{0i}) and the viscous constant (η), using a tribometer [18-26]. The tribometer used and the approach followed in this study are those used by T.T. Ngo [22].

This tribometer is composed of an inner cylinder, with a diameter of 10.7 cm and a height of 10 cm, and a container with a diameter equal to 30 cm and a height of 20 cm (Fig. 5). This device is based on the principle of coaxial cylinders where the internal cylinder rotates relative to the external container by imposed rotation speeds according to the profile defined in Fig. 6c. The tribological test consists of two measurements. The first one is carried out by filling half of the container with concrete (Fig. 6a) and the second one is done by completely filling the container with concrete (Fig. 6b).

At each instant of the test, the control software records the torque T corresponding to a speed V . The result obtained is in the form of a torque-rotation speed diagram of the cylinder, according to eq. (6), as shown in Fig. 6d.

$$T = T_0 + kV \quad (6)$$

Where T (N.m) is the applied torque to the revolving cylinder; T_0 (N.m) is the initial torque; k (N.m.s/rad) is the linear coefficient and V (tr/min) is the cylinder rotating speed.

Table 3 - The surfaces area of gravel.

1	2	3	4	5	6	7	8	9	10	11
T_{m_i}	T_{M_i}	d_i	Mu_i (kg)	v_i (m^3)	S_i (m^2)	ω (m^3/kg)	V_i (m^3)	N_i	S_i (m^2)	SD_G (m^2)
0	0,08	0,04	0,0072	$3,351 \times 10^{-14}$	$5,027 \times 10^{-09}$	0,000391	$2,82 \times 10^{-06}$	84004837,62	0,422	
0,08	0,16	0,12	0,001	$9,048 \times 10^{-13}$	$4,524 \times 10^{-08}$	0,000391	$3,91 \times 10^{-07}$	432123,65	0,019	
0,16	0,315	0,2375	0,0057	$7,014 \times 10^{-12}$	$1,772 \times 10^{-07}$	0,000391	$2,23 \times 10^{-06}$	317713,59	0,056	
0,315	3,15	0,4725	0,0069	$5,523 \times 10^{-11}$	$7,014 \times 10^{-07}$	0,000391	$2,69 \times 10^{-06}$	48842,223	0,034	
3,15	4	3,575	0,0094	$2,392 \times 10^{-08}$	$4,015 \times 10^{-05}$	0,000391	$3,67 \times 10^{-06}$	153,621	0,006	
4	5	4,5	0,0625	$4,771 \times 10^{-08}$	$6,362 \times 10^{-05}$	0,000391	$2,44 \times 10^{-05}$	512,146	0,032	0,748
5	6,3	5,65	0,0931	$9,444 \times 10^{-08}$	0,0001003	0,000391	$3,64 \times 10^{-05}$	385,439	0,038	
6,3	8	7,15	0,0957	$1,914 \times 10^{-07}$	0,0001606	0,000391	$3,74 \times 10^{-05}$	195,499	0,031	
8	10	9	0,1175	$3,817 \times 10^{-07}$	0,0002545	0,000391	$4,59 \times 10^{-05}$	120,354	0,031	
10	12,5	11,25	0,0958	$7,455 \times 10^{-07}$	0,0003976	0,000391	$3,746 \times 10^{-05}$	50,241	0,019	
12,5	16	14,25	0,0749	$1,515 \times 10^{-06}$	0,0006379	0,000391	$2,928 \times 10^{-05}$	19,328	0,012	
16	20	18	0,336	$3,054 \times 10^{-06}$	0,0010179	0,000391	0,0001314	43,020	0,044	

Table 4 - The surfaces area of sand.

1	2	3	4	5	6	7	8	9	10	11
T_{m_i}	T_{M_i}	d_i	Mu_i (kg)	v_i (m^3)	S_i (m^2)	ω (m^3/kg)	V_i (m^3)	N_i	S_i (m^2)	SD_G (m^2)
0	0,08	0,04	0,139	$3,35 \times 10^{-14}$	$5,027 \times 10^{-09}$	0,0003704	$5,14 \times 10^{-05}$	1534076813	7,711	
0,08	0,16	0,12	0,075	$9,05 \times 10^{-13}$	$4,524 \times 10^{-08}$	0,0003704	$2,76 \times 10^{-05}$	30537445	1,381	
0,16	0,315	0,2375	0,042	$7,01 \times 10^{-12}$	$1,772 \times 10^{-07}$	0,0003704	$1,55 \times 10^{-05}$	2207105,3	0,391	
0,315	0,63	0,4725	0,166	$5,52 \times 10^{-11}$	$7,014 \times 10^{-07}$	0,0003704	$6,16 \times 10^{-05}$	1114456,7	0,782	
0,63	1,25	0,94	0,0995	$4,35 \times 10^{-10}$	$2,776 \times 10^{-06}$	0,0003704	$3,69 \times 10^{-05}$	84737,79	0,235	10,989
1,25	2,5	1,875	0,3238	$3,45 \times 10^{-09}$	$1,104 \times 10^{-05}$	0,0003704	$1,199 \times 10^{-04}$	34746,466	0,384	
2,5	3,15	2,825	0,02	$1,18 \times 10^{-08}$	$2,507 \times 10^{-05}$	0,0003704	$7,407 \times 10^{-06}$	627,498	0,016	
3,15	4	3,575	0,1028	$2,39 \times 10^{-08}$	$4,015 \times 10^{-05}$	0,0003704	$3,807 \times 10^{-05}$	1591,485	0,064	
4	5	4,5	0,0498	$4,77 \times 10^{-08}$	$6,362 \times 10^{-05}$	0,0003704	$1,844 \times 10^{-05}$	386,571	0,025	
5	6,3	5,65	0	$9,44 \times 10^{-08}$	0,0001003	0,0003704	0	0	0	

The transition from the torque-rotation speed obtained with the tribometer to the interface law described in eq. (7) is carried out by eqs. (8), (9) and (10) taking into account the geometry of the device (Fig. 6d).

$$\tau = \tau_{oi} + \eta v \tag{7}$$

$$\tau_{oi} = \frac{T_0}{2\pi r^2 h} \tag{8}$$

$$\eta = \frac{k}{(2\pi)^2 r^3 h} \tag{9}$$

$$v = \omega \cdot 2\pi r \tag{10}$$

Where τ (Pa) is the shear stress, τ_{oi} (Pa) the interface yield stress, η (Pa. s/m) the viscous constant and v (m/s) the rotation speed, r (m) is the mean radius of the cylinder, T_0 (N.m) is the measured torque and h (m) is the height of the cylinder.

Table 5 - The constituents of CM and CEM mortars tested.

		Cement (Kg/m³)	Limestone fillers (Kg/m³)	Blast furnace slag (Kg/m³)	Sand (Kg/m³)	Superplasticizer (Kg/m³)	Water (Kg/m³)
Concrete equivalent mortar	CEMT	622	0	0	1306	3,11	311
	CEM1	560	62	0	1306	3,11	311
	CEM2	497	125	0	1306	3,11	311
	CEM3	435	187	0	1306	3,11	311
	CEM4	497	0	125	1306	3,11	311
	CEM5	373	0	249	1306	3,11	311
	CEM6	249	0	373	1306	3,11	311
Concrete mortar	CMT	654	0	0	1234	3,27	327
	CM1	588,2	65,4	0	1234	3,27	327
	CM2	523	131	0	1234	3,27	327
	CM3	458	196	0	1234	3,27	327
	CM4	523	0	131	1234	3,27	327
	CM5	392	0	262	1234	3,27	327
	CM6	262	0	392	1234	3,27	327

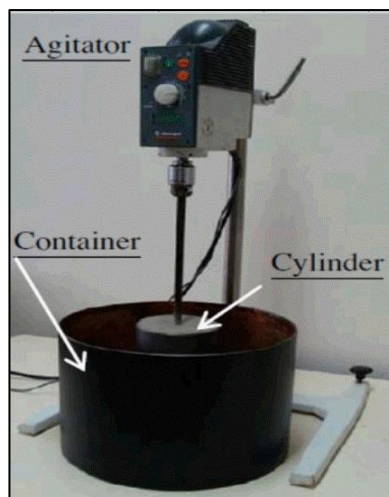


Fig. 5– Principal parts of tribometer[27].

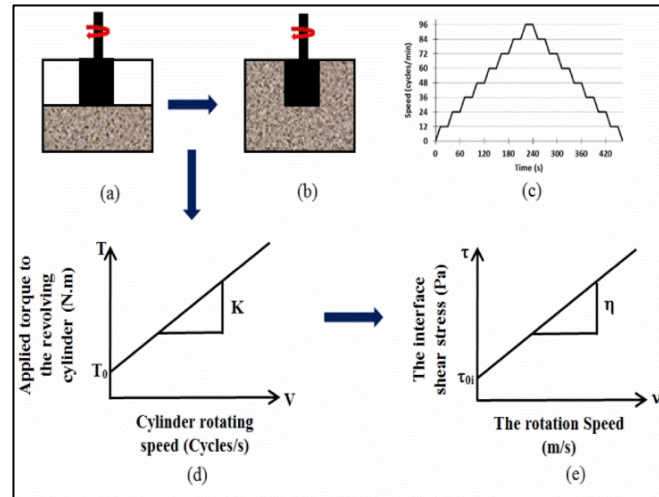


Fig.6–The tribometric measurement approach developed by [22].

2.3 Characterization tests of the mortars under study

2.3.1 Slump test

The slump of the mortars under study was measured using a mini-cone whose dimensions are smaller than those of Abrams cone, with a homothetic ratio equal to two (Fig. 7).

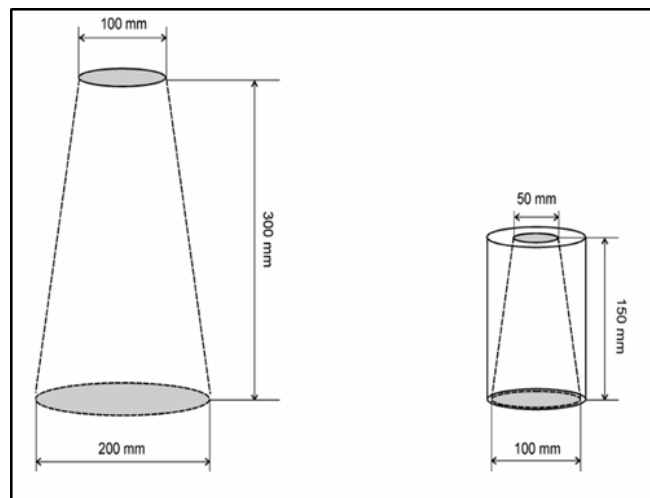


Fig.7–The Abrams cone and the mini-cone [9].

2.3.2 Rheological test

The rheological behavior of concrete and mortar in the fresh state is that of a Binghamian fluid. It is characterized by two properties, namely the yield stress (τ_0) and the plastic viscosity (μ), which means that the relationship between the shear rate and shear velocity is linear [28,29]. These two properties may be determined using rheometric tests [30-34].

The rheological properties identified in this study were determined by the same type of rheometer as that developed by [44]. This type of quilt rheometer is made up of a specific mortar container that is characterized by a diameter of 50mm and height of 130mm, with a blade of 25mm in diameter and height of 100mm (Fig. 8).

The operating principle of the rheometer initially consists in rotating, at different speeds, a cross-shaped blade in the empty container (Fig. 9a). This blade is then rotated in a cylindrical sample of fresh concrete (Fig. 9b). The speed profile adopted for the rheometer tests is presented in Fig. 9c.

During the two stages, the rotational torques (M) exerted to keep the blade in rotation are measured. Each torque corresponds to an imposed rotation speed (Ω). This torque is recorded by the agitator control software.

The relationship between the torque and rotational speed, presented in Fig. 9d, is in the form of a linear function (eq. (11)).

$$M = M_0 + \kappa\Omega \tag{11}$$

Where M is the total torque applied to keep the blade in rotation (N.m), M_0 is torque at the origin (N.m), Ω is the blade rotation speed (tours/s), κ is a coefficient of proportionality. The rheological parameters, described in Bingham's model (eq. (12)), are determined using the eqs. (13), (14), (15) (16) developed by P. Estellé et al [45] and P. Nanthagopalan et al [46] while taking into account the experimental data on torque and rotational speed ($M_i - \Omega_i$) (Fig. 9e).

$$\tau = \tau_0 + \mu\dot{\gamma} \tag{12}$$

Where τ_0 is the yield stress (Pa), μ is the plastic viscosity (Pa.s) et $\dot{\gamma}$ is the shear rate gradient (s^{-1}).

$$\dot{\gamma}_1 = 2 \cdot M \frac{d\Omega}{dM} \tag{13}$$

$$\dot{\gamma}_2 = 2 \frac{M \frac{d\Omega}{dM}}{\left(1 - \frac{R_b^2}{R_c^2}\right)} - \frac{\Omega - M \frac{d\Omega}{dM}}{\ln\left(\frac{R_b}{R_c}\right)} \tag{14}$$

Where R_b (m) is the radius of the blade, R_c (m) the radius of the container, $\frac{d\Omega}{dM}$ is the value of the derivative of the blade rotation speed by its torque can be approximated by eq. (15). The shear rate ($\dot{\gamma}$) generated by a rotation speed Ω_i represents the maximum value between ($\dot{\gamma}_1$) and ($\dot{\gamma}_2$).

$$\frac{d\Omega}{dM} \cong \frac{\Omega_j - \Omega_{j-1}}{M_j - M_{j-1}} \tag{15}$$

In addition, the shear stress is determined by eq. (16).

$$\tau_i = \frac{1}{2}(\tau_{j-1} + \tau_{j+1}) \tag{16}$$

Where

$$\tau_j (M) = \frac{M_j}{2 \pi h R_b^2} \tag{17}$$

Where h (m) is the height of the blade. After the determination of the shear stress (τ_i) and the shear rate ($\dot{\gamma}$) we can estimate the rheological properties of the mortar (τ_0, μ).



Fig. 8–The components of the rheometer.

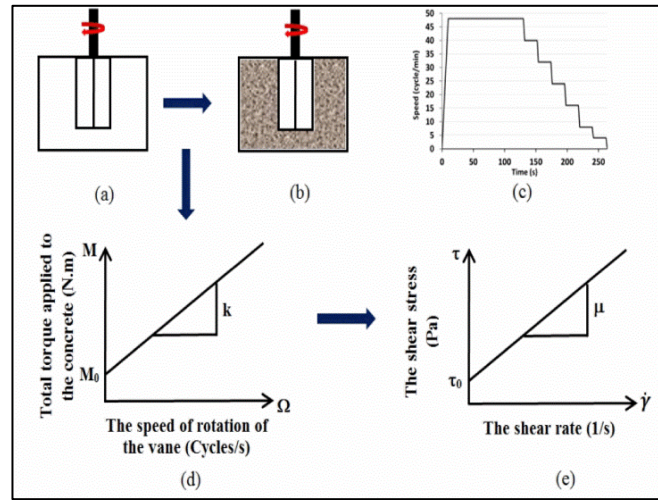


Fig. 9–The rheological measurement process developed by [41].

3 Results and discussion

3.1 Correlation between concrete slump and the corresponding mortars

The correlative study between the concrete slump and the spread flow of associated mortars has shown that there is a linear relationship between the slump of concrete and the spread flow of its concrete equivalent mortar (CEM), with a coefficient of determination equal to 0.807 for the mixtures containing limestone fillers (Fig. 10a), and a coefficient of determination equal to 0.985 for those containing the blast furnace slag. On the other hand, the correlation between the slump of concrete and the spread flow of its concrete mortars (CMs) is not satisfactory for all mixes (Fig. 11).

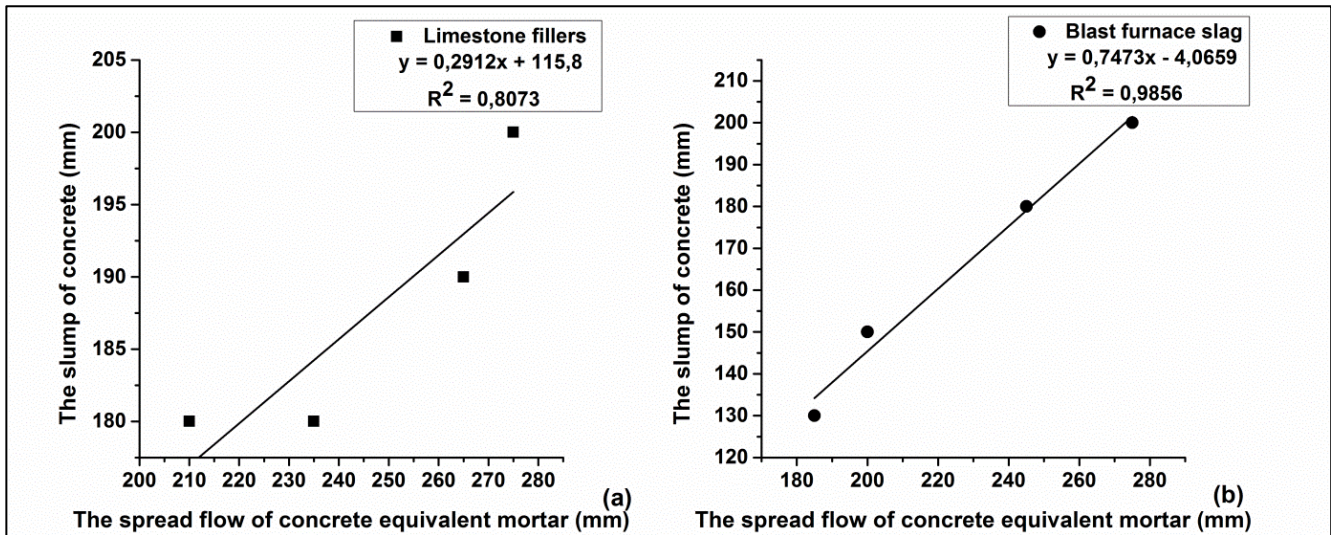


Fig. 10 –Relationship between the slump of concrete and the spread flow of CEM: (a) samples containing limestone fillers, (b) samples containing blast furnace slag.

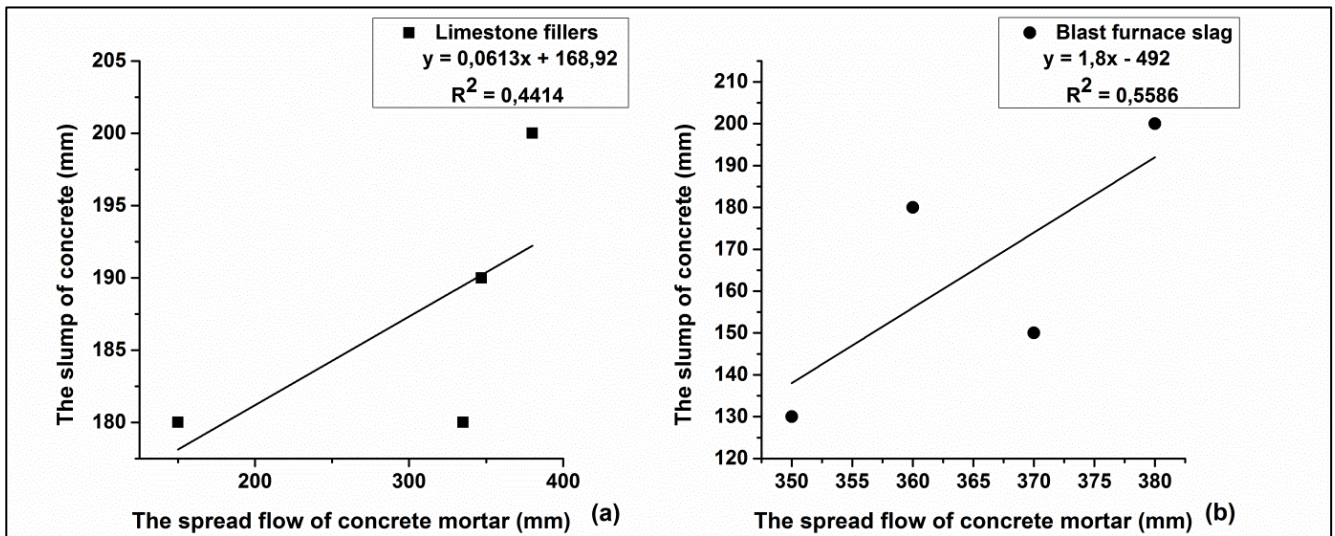


Fig. 11 –Relationship between the slump of concrete and the spread flow of CM: (a) samples containing limestone fillers, (b) samples containing blast furnace slag.

3.2 Correlation between the rheology of concrete mortar and tribology of concrete

Figures 12 and 13 make it possible to note that the determination coefficients R^2 obtained are very low and therefore no link can be established between the tribological and rheological parameters of the mixtures tested. This may be due to the amount of gravel removed, which affects the internal friction in concrete mortars (CM).

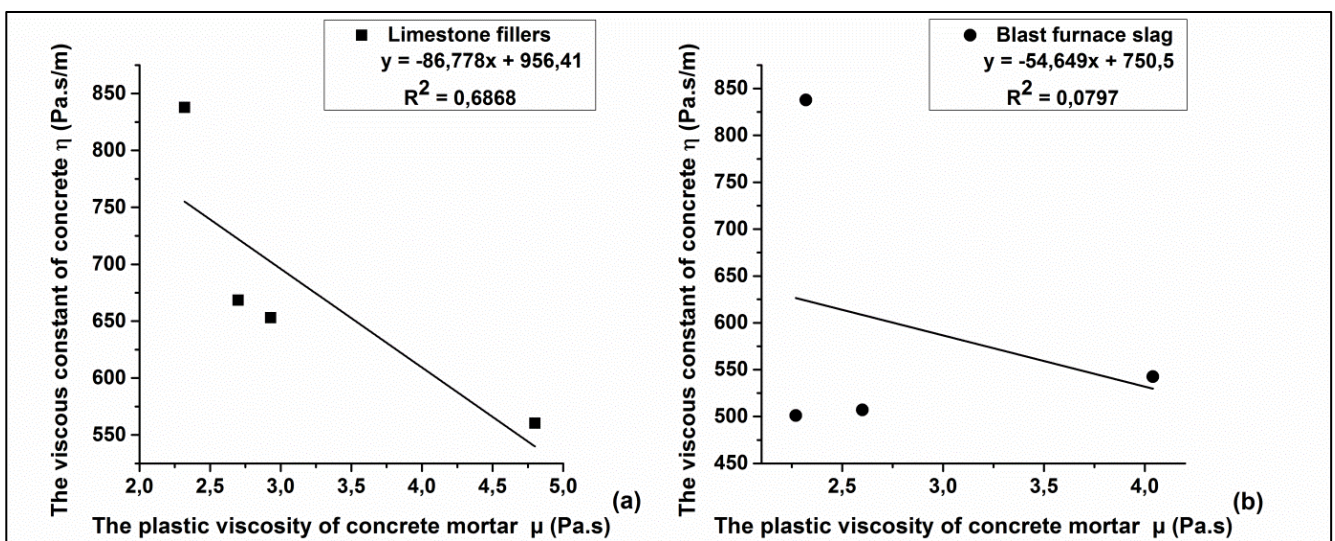


Fig. 12–Relationship between the viscous constant of concrete and the plastic viscosity of CM: (a) samples containing limestone fillers, (b) samples containing blast furnace slag.

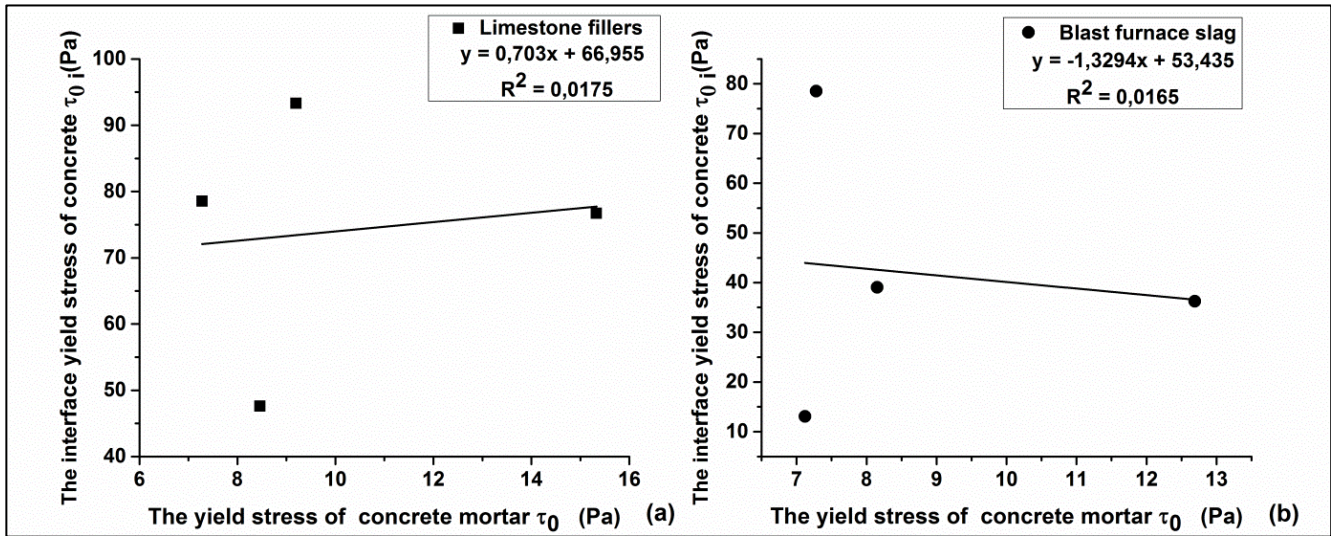


Fig. 13 –Relationship between the interface yield stress of concrete and the yield stress of CM: (a) samples containing limestone fillers, (b) samples containing blast furnace slag.

3.3 Correlation between the rheology of concrete equivalent mortar and the tribology of concrete

Figures 14 and 15 shows that there is a better correlation between the tribology of concrete and the rheology of the corresponding CEMs. In addition, it seems that the behaviors of the two materials (concrete and mortar) are almost identical. This may result from the addition of a quantity of sand having the same granular surface as that of the removed gravel. According to [9], the importance of adding sand to have the same granular surface in concrete as in the concrete equivalent mortar lies in the fact that the quantities of paste and sand that adhere to gravel are proportional to the granular surface of gravel.

It is important to note also that the rheological parameters of concrete equivalent mortar have a significant influence on the tribology of concrete as compared to that of concrete mortar. This may certainly be attributed to the higher dosage of sand in concrete equivalent mortars (CEMs) than in concrete mortars (CMs), as presented in Table 5. This would lead to a higher dosage of fines in sand, which increases, on the one hand, the need for water [47] and on the other hand, the demand for superplasticizer in order to maintain the workability [48]. Consequently, the fluidity of CEMs decreases and the rheological parameters increase, which means that both the rheology and tribology of concrete go up. It is for this reason that no correlation was detected between the properties of concrete and those of the corresponding concrete mortar.

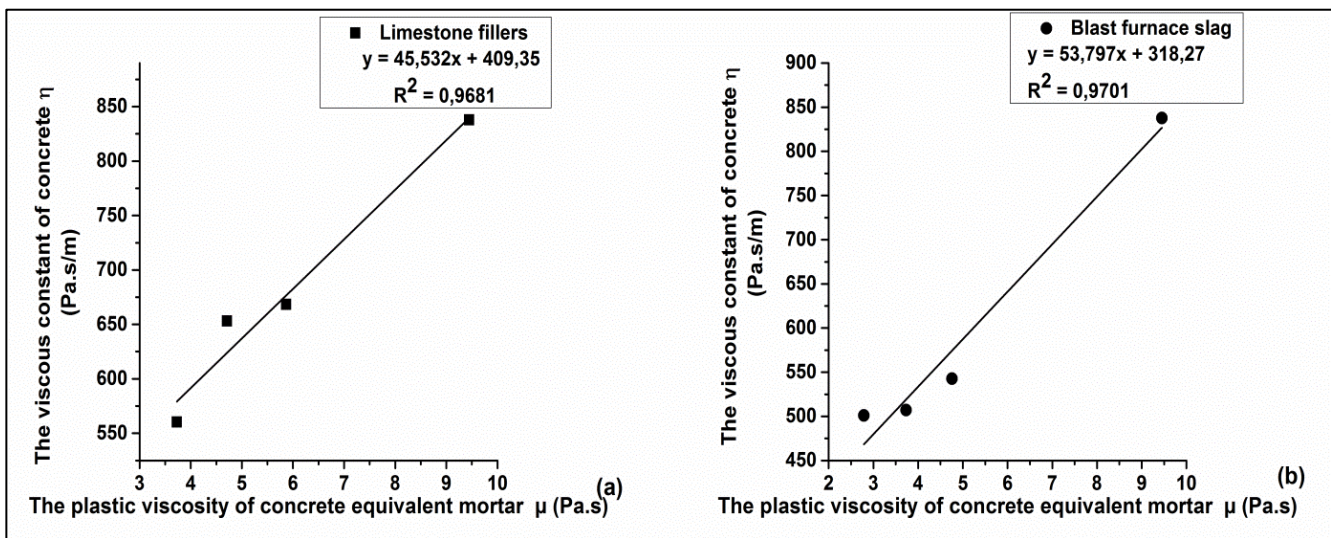


Fig. 14 –Relationship between the viscous constant of concrete and the plastic viscosity of CEM: (a) samples containing limestone fillers, (b) samples containing blast furnace slag.

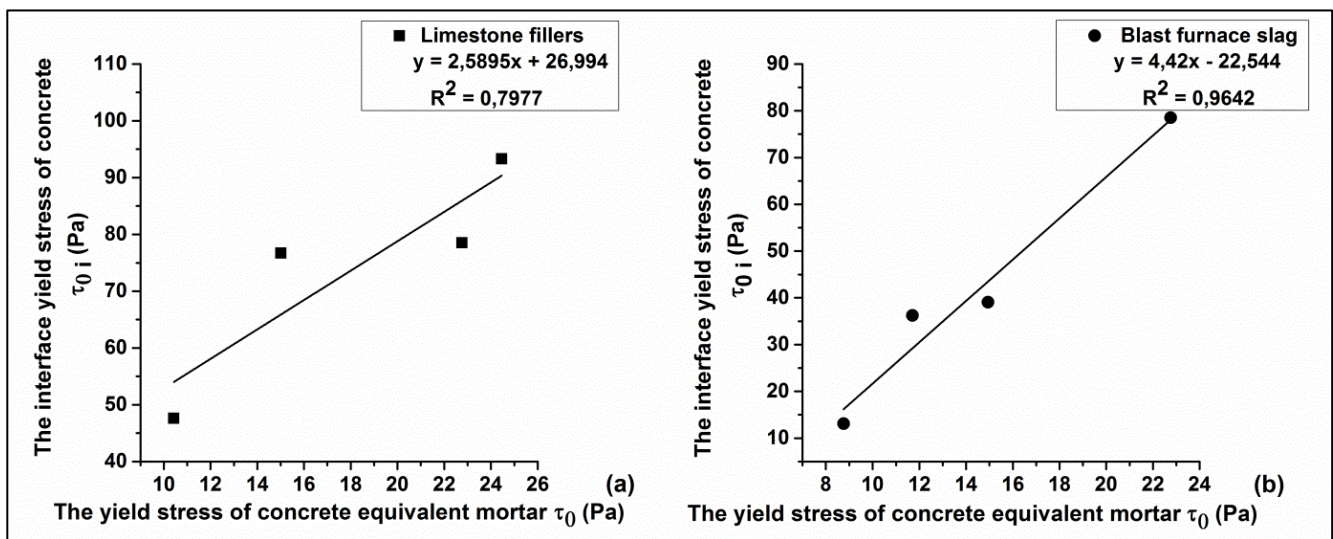


Fig. 15 –Relationship between the interface yield stress of concrete and the yield stress of CEM: (a) samples containing limestone fillers, (b) samples containing blast furnace slag.

4 Conclusions

Owing to the fact that concrete is a material that is heavier than mortar, it was found useful to use rapid testing methods that can provide results correlable with those obtained on concrete.

To address this problem, it was decided to combine the tribological measurements of concrete with the rheological measurements of two types of mortar, namely conventional concrete mortars (CM) and concrete equivalent mortars (CEMs). The satisfactory correlations have been existed between the behavior of concrete in the fresh state and its corresponding CEM for all of the mixtures under study. Hence, a linear relationship has been established between the slump of concrete and the spread flow of the associated concrete equivalent mortars (CEMs), with coefficients of determination equal to 0.807 and 0.985, respectively, for mixtures containing limestone fillers and those containing blast furnace slag.

In addition, a better correlation was found between the tribological parameters of concrete and the rheological parameters of CEMs, with very high determination coefficients. However, no correlation was found between the behavior of concrete in the fresh state and its corresponding concrete mortar (CM), for all the mixtures studied, which allows us to conclude that the tribology of concrete is influenced much more by the rheology of the corresponding concrete equivalent mortars (CEMs) than by that of concrete mortars (CMs). This may be due to the composition of CEMs which consists of replacing the gravel with a certain quantity of sand having the same granular surface.

REFERENCES

- [1]- P. Banfill, The rheology of fresh mortar. *Mag. Concr. Res.* 43 (1991) 13–21. doi:10.1680/mac.1991.43.154.13
- [2]- A. Yahia, M. Tanimura, A. Shimabukuro, Y. Shimovama, Effect of rheological parameters on self-compatibility of concrete containing various mineral admixtures. In proceeding of 1st International RILEM symposium on self-compacting concrete, Stockholm, Sweden, 1999, pp. 523–535.
- [3]- P. Billberg, Fine mortar rheology in mix design of SCC. In: Proceedings of 1st International RILEM Symposium on Self-compacting Concrete, Stock, Sweden, 1999, pp. 47–58.
- [4]- J. E. Wallevik, Rheology of Particle Suspensions - Fresh Concrete, Mortar and Cement Paste with Various Types of Lignosulfonates, PhD Thesis, University of Science and Technology, Norway, 2003.
- [5]- H. Okamura, M. Ouchi, Self-compacting concrete. *J. Adv. Concr. Technol.* 1(1) (2003) 5–15. doi:10.3151/jact.1.5
- [6]- M. Lamechi, K.M.A. Hossain, R. Patel, M. Shehata, N. Bouzoubaâ, Influence of paste/mortar rheology on the flow characteristics of high-volume fly ash self-consolidating concrete. *Mag. Concr. Res.* 59 (2007) 517–528. doi:10.1680/mac.2007.59.7.517
- [7]- I.Y.T. Ng, P.L. Ng, A.K.H. Kwan, Rheology of mortar and its influences on performance of self-consolidating concrete. *Key Eng. Mater.* 400-402 (2008) 421-426. doi:10.4028/www.scientific.net/KEM.400-402.421

- [8]- H. Paiva, A. Velosa, P. Cachim, V.M. Ferreira, Correlation between mortar and concrete behavior using rheological analysis. *J. Build. Eng.* 4 (2015) 177–188. doi:10.1016/j.jobee.2015.09.001
- [9]- A. Schwartzentruber, C. Catherine, Method of Concrete Equivalent Mortar—A Novel Tool to Help in Formulation of Concrete with Admixtures. *Mater. Struct.* 33(8) (2000) 475-482.
- [10]- J. Assaad, K.H. Khayat, Assessment of thixotropy of self- consolidating concrete and concrete-equivalent-mortar – Effect of binder composition and content. *ACI Mater. J.* 101(5) (2004) 400 – 408.
- [11]- J. Assaad, D. Yehia, Use of the equivalent mortar phase to assess thixotropy of fresh scc – prediction of interfacial bond strength between successive placement lifts. *Appl. Rheol.* 26 (2016) 42759. doi:10.3933/applrheol-26-42759
- [12]- T.K. Erdem, K.H. Khayat, A. Yahia, Correlating rheology of self-consolidating concrete to corresponding concrete-equivalent mortar. *ACI Mater. J.* 106(2) (2009) 154-160.
- [13]- D. Kabagire, P. Diederich, A. Yahia, New insight into the equivalent concrete mortar approach for self- consolidating concrete. *J. Sustainable Cement Based Mater.* 4 (2015) 215-224. doi :10.1080/21650373.2015.1018983
- [14]- H. D. Le, Etude de l'effet de la couche limite sur les profils de vitesses du béton pompé, Ph.D. Thesis, University of Cergy-Pontoise, 2014.
- [15]- M. Adjoudj, K. Ezziane, E.H. Kadri, T.T. Ngo, A. Kaci, Evaluation of rheological parameters of mortar containing various amounts of mineral addition with polycarboxylate superplasticizer. *Constr. Build. Mater.* 70 (2014) 549-559. doi:10.1016/j.conbuildmat.2014.07.111
- [16]- J. G. Jawahar, C. Sashidhar, I. V. Ramana Reddy, J. Annie Peter, Optimization of superplasticiser and viscosity modifying agent in self-compacting mortar. *Asian J. Civ. Eng.* 14(1) (2013) 71-86.
- [17]- S.M.A. BoukliHacene, F. Ghomari, F. Schoefs, A. Khelidj, Probabilistic modelling of compressive strength of concrete using response surface methodology and neural networks. *Arabian J. Sci. Eng.* 39(6) (2014) 4451-4460. doi:10.1007/s13369-014-1139-y
- [18]- B. Chouinard, Etude des relations entre la rhéologie du béton et sa Pompabilité, PhD Thesis, University of Laval, 1999.
- [19]- D. Kaplan, Pompage des bétons, PhD Thesis, Ecole Central des Ponts et Chaussées, 2000.
- [20]- D. Kaplan, F. D. Larrard, T. Sedran, Design of concrete pumping circuit. *ACI Mater. J.* 102 (2) (2005) 110–117.
- [21]- F. Chapdelaine, Étude fondamentale et pratique sur le pompage du béton, PhD Thesis, University of Laval, 2007.
- [22]- T.T. Ngo, Influence de la composition des bétons sur les paramètres de pompage et validation d'un modèle de prévision de la constante visqueuse, PhD Thesis, University of Cergy Pontoise, 2009.
- [23]- T.T. Ngo, E.H. Kadri, F. Cussigh, R. Bennacer, Measurement and modeling of fresh concrete viscous constant to predict pumping pressures. *Can. J. Civ. Eng.* 38 (2011) 944–956. doi:10.1139/111-058
- [24]- S. H. Kwon, C. K. Park, J. H. Jeong, S. D. Jo, S. H. Lee, Prediction of Concrete Pumping-Part I: Development of New Tribometer for Analysis of Lubricating Layer. *ACI Mater. J.* 110 (6) (2013) 647-655.
- [25]- D. Feys, K. H. Khayat, A. Perez-Schell, R. Khatib, Development of a tribometer to characterize lubrication layer properties of self-consolidating concrete. *Cement Concrete Res.* 54 (2014) 40–52. doi:10.1016/j.cemconcomp.2014.05.008
- [26]- H. Li, D. Sun, Z. Wang, F. Huang, Z. Yi, and al., A Review on the Pumping Behavior of Modern Concrete. *J. Adv. Concr. Technol.* 18 (2020) 352-363. doi:10.3151/jact.18.352
- [27]- T.T. Ngo, E.H. Kadri, F. Cussigh, R. Bennacer, Relationships between concrete composition and boundary layer composition to optimize concrete pumpability. *Eur. J. Environ. Civ. Eng.* 16 (2012) 157-177. doi:10.1080/19648189.2012.666910
- [28]- S.E. Chidiac, F. Mahmoodzadeh, Constitutive flow models for characterizing the rheology of fresh mortar and concrete. *Can. J. Civ. Eng.* 40 (2013) 475-482. doi: 10.1139/L2012-025
- [29]- L. Guoming, C. Weimin, C. Lianjun, P. Gang, L. Zhaoxia, Rheological properties of fresh concrete and its application on shotcrete. *Constr. Build. Mater.* 243 (2020) 118-180. doi:10.1016/j.conbuildmat.2020.118180
- [30]- C. Ferraris, F. De Larrard, Testing and Modelling of Fresh Concrete Rheology. NIST Interagency/Internal Report (NISTIR) 6094, National Institute of Standards and Technology, 1998. doi:10.6028/NIST.IR.6094
- [31]- F. De Larrard, T. Sedran, Mixture-proportioning of high-performance concrete *Cement Concrete Res.* 32(11) (2002) 1699-1704. doi:10.1016/S0008-8846(02)00861-X
- [32]- J. Golaszewski, J. Szwabowski, Influence of superplasticizer on rheological behaviour of fresh cement mortars. *Cement Concrete Res.* 34(2) (2003) 235-248. doi:10.1016/j.cemconres.2003.07.002
- [33]- J. E. Wallevik, Relationship between the Bingham parameters and slump. *Cement Concrete Res.* 36(7) (2006) 1214-1221. doi:10.1016/j.cemconres.2006.03.001

- [34]- P. Estellé, C. Lanos, High torque vane rheometer for concrete: Principal and validation from rheological measurements. *Appl. Rheol.* 22 (2012) 12881. doi:10.3933/AppIRheol-22-12881
- [35]- E. Koehler, D. Fowler, C. Ferraris, S. Amziane, New portable rheometer for fresh self-consolidating concrete. *ACI Mater. J.* 233 (2006) 97-116.
- [36]- C. Lanos, P. Estellé, Vers une réelle rhéométrie adaptée aux bétons frais. *Eur. J. Environ. Civ. Eng.* 13(4) (2009) 457-471. doi:10.1080 / 19648189.2009.9693123
- [37]- A. Kaci, M. Chaouche, P.A. Andréani, H. Brossas, Rheological behaviour of render mortars. *Appl. Rheol.* 19 (2009) 13794. doi:10.1515/arh-2009-0004
- [38]- A.I. Laskar, S. Talukdar, Rheology-based approach for workability characterization of high-performance concrete. *Can. J. Civ. Eng.* 36 (2009) 1239–1244. doi:10.1139/L09-058
- [39]- J. Wen-Chen, Y. Ching-Ting, Development of a modified concrete rheometer to measure the rheological behavior of conventional and self-consolidating concretes. *Cement Concrete Comp.* 32(6) (2010) 450-460. doi:10.1016/j.cemconcomp.2010.01.001
- [40]- M. Choi, N. Roussel, K. Youngjin, J. Kim, Lubrification layer properties during concrete pumping. *Cement Concrete Res.* 45 (2013) 69-78. doi:10.1016/j.cemconres.2012.11.001
- [41]- H. Soualhi, Optimisation de la viscosité des bétons à faible impact environnemental. PhD Thesis, University of Cergy pontoise, 2014.
- [42]- M. Adjoudj, Effet des additions minérales et organiques sur le comportement rhéologique du béton. PhD Thesis, University of Chlef, 2015.
- [43]- O. Taleb, F. Ghomari, M.A BoukliHacene, E.H. Kadri, H. Soualhi, Formulation and rheology of eco-self-compacting concrete (Eco-SCC). *J. Adhes. Sci. Technol.* 31 (3) (2017) 272-296. doi:10.1080/01694243.2016.1215010
- [44]- H. Soualhi, E.H. Kadri, T.T. Ngo, A. Bouvet, F. Cussigh, S. Kenai, A Vane Rheometer for Fresh Mortar: Development and Validation. *Appl. Rheol.* 24 (2014) 22594. doi:10.3933 / APPLRHEOL-24-22594
- [45]- P. Estellé, C. Lanos, A. Perrot, Processing the Couetteviscometry data using a Bingham approximation in shear rate calculation. *J. Non-Newtonian Fluid.* 154 (2008) 31–38. doi:10.1016/j.jnnfm.2008.01.006
- [46]- P. Estellé, C. Lanos, A. Perrot, S. Amziane, Processing the vane shear flow data from Couette analogy. *Appl. Rheol.* 18(3) (2008) 34–37. doi:10.3933/AppIRheol-18-34037
- [47]- P. Nanthagopalan, M. Santhanam, Fresh and hardened properties of self-compacting concrete produced with manufactured sand. *Cement Concrete Comp.* 33 (2011) 353 – 358. doi:10.1016/j.cemconcomp.2010.11.005
- [48]- O. Taleb, F. Ghomari, M.A. BoukliHacene, M. Henaoui and H. Soualhi, Experimental and Numerical Analysis of the Rheology of Self-compacting Concrete Using a Vane Rheometer. *Jordan J. Civ. Eng.* 15(1) (2021) 116-132.